The Optics of the Low Energy FFAG cell of the eRHIC collider, using realistic field maps

N. Tsoupas, S. Brooks, A. Jain, G. Mahler, F. Meot, V. Ptitsyn, D. Trbojevic, BNL
M. Severance, SBU

Schematic diagram of the eRHIC accelerator

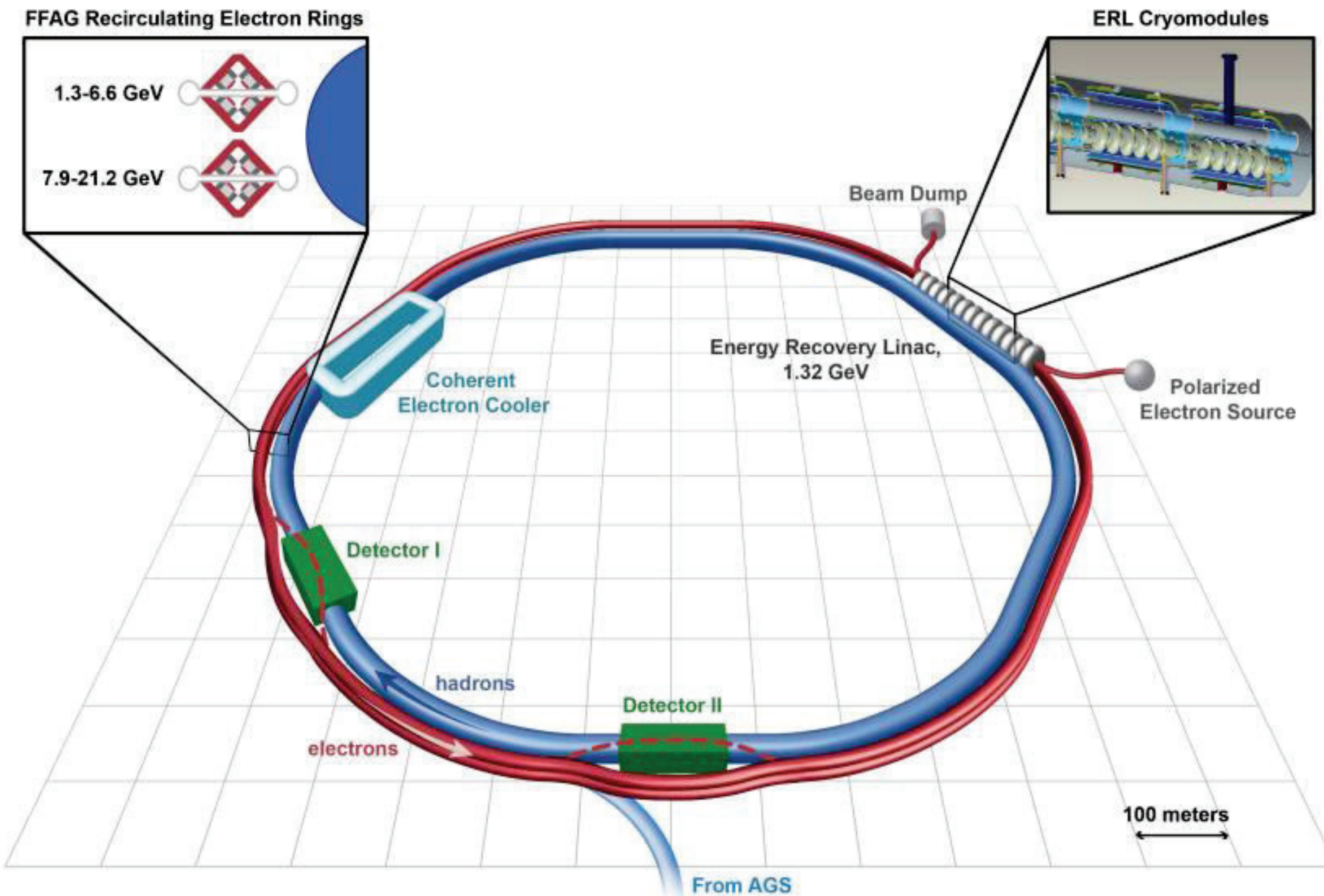

FFAG Cell structure of the eRHIC

Energy of e-bunches circulating in Low Energy ring 1.32, 2.64, 3.96, 5.28, 6.6 GeV

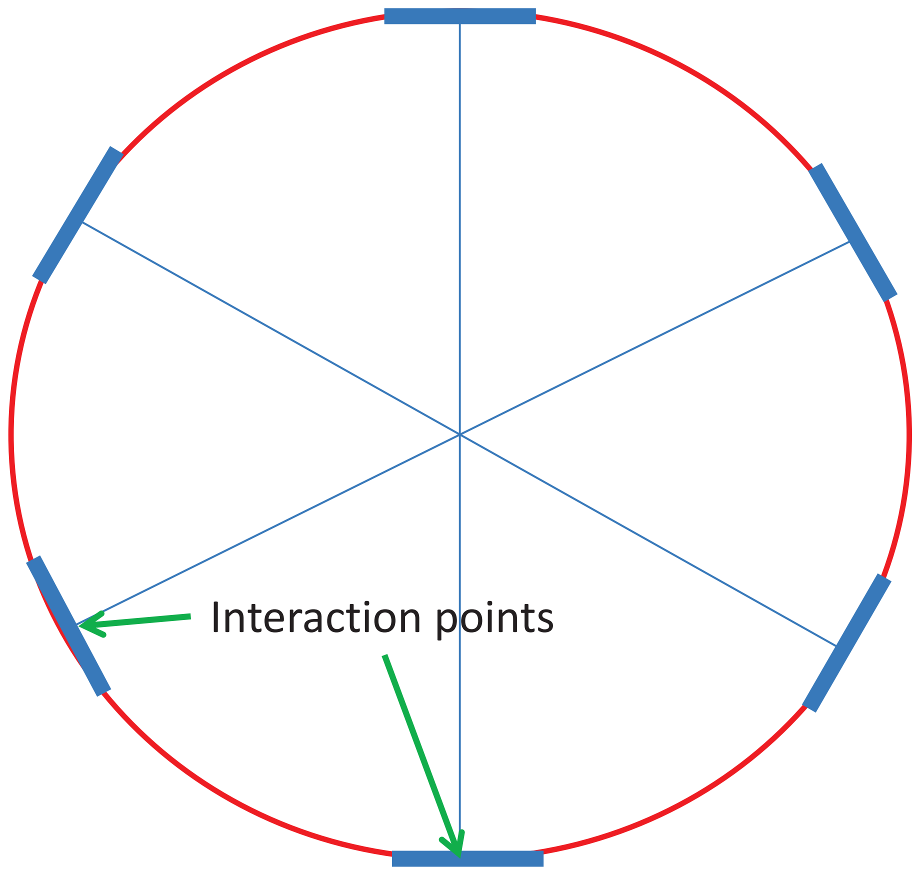

212 cells per sextant

FFAG Cell of the eRHIC

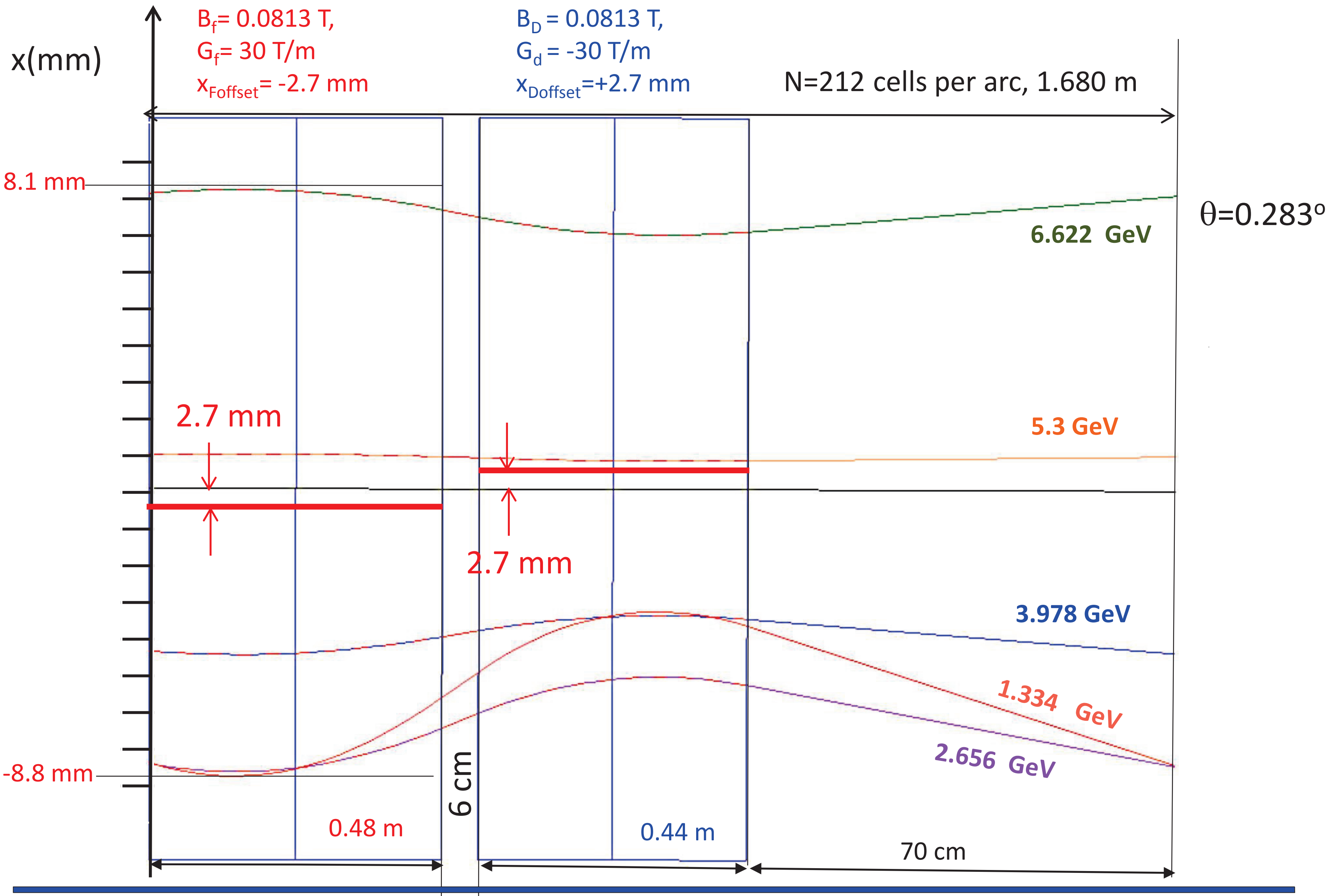

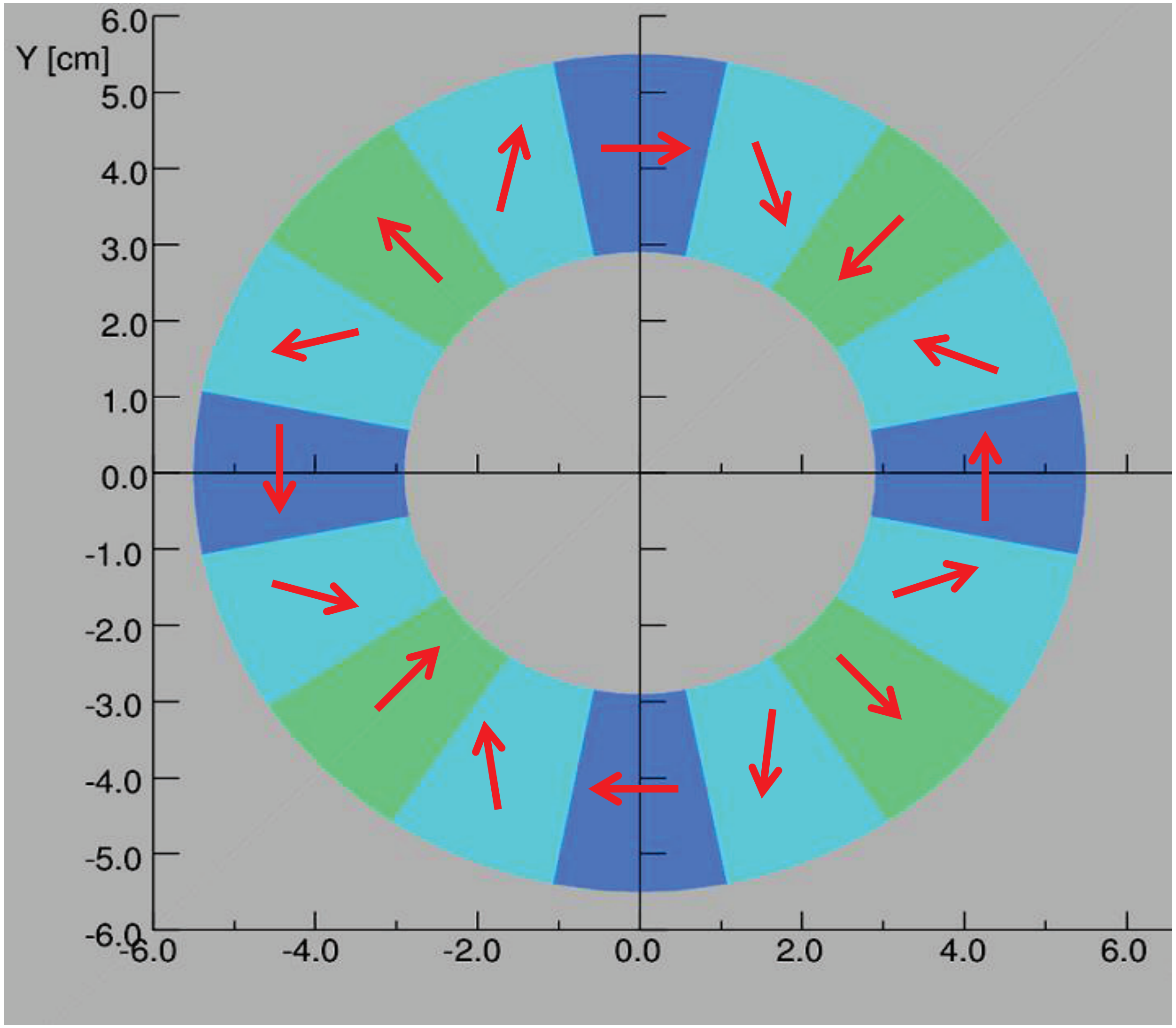
Y [cm]
6.0
5.0
4.0
3.0
2.0
1.0
0.0
-1.0
-2.0
-3.0
-4.0
-5.0
-6.0
-6.0
-4.0
-2.0
0.0
2.0
4.0
6.0

Perm. Magnet Material SmCO

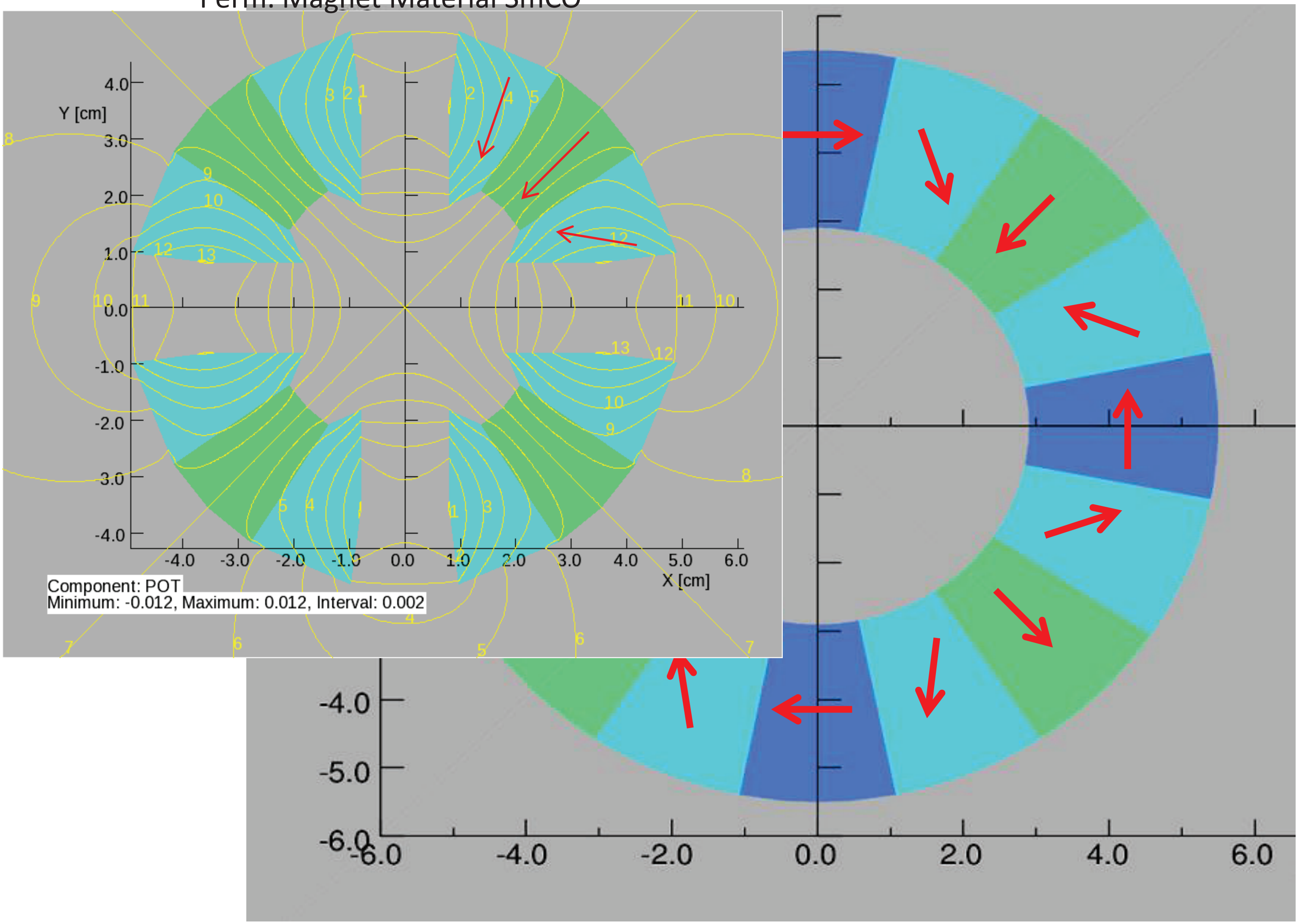

Perm. Magnet Material SmCO

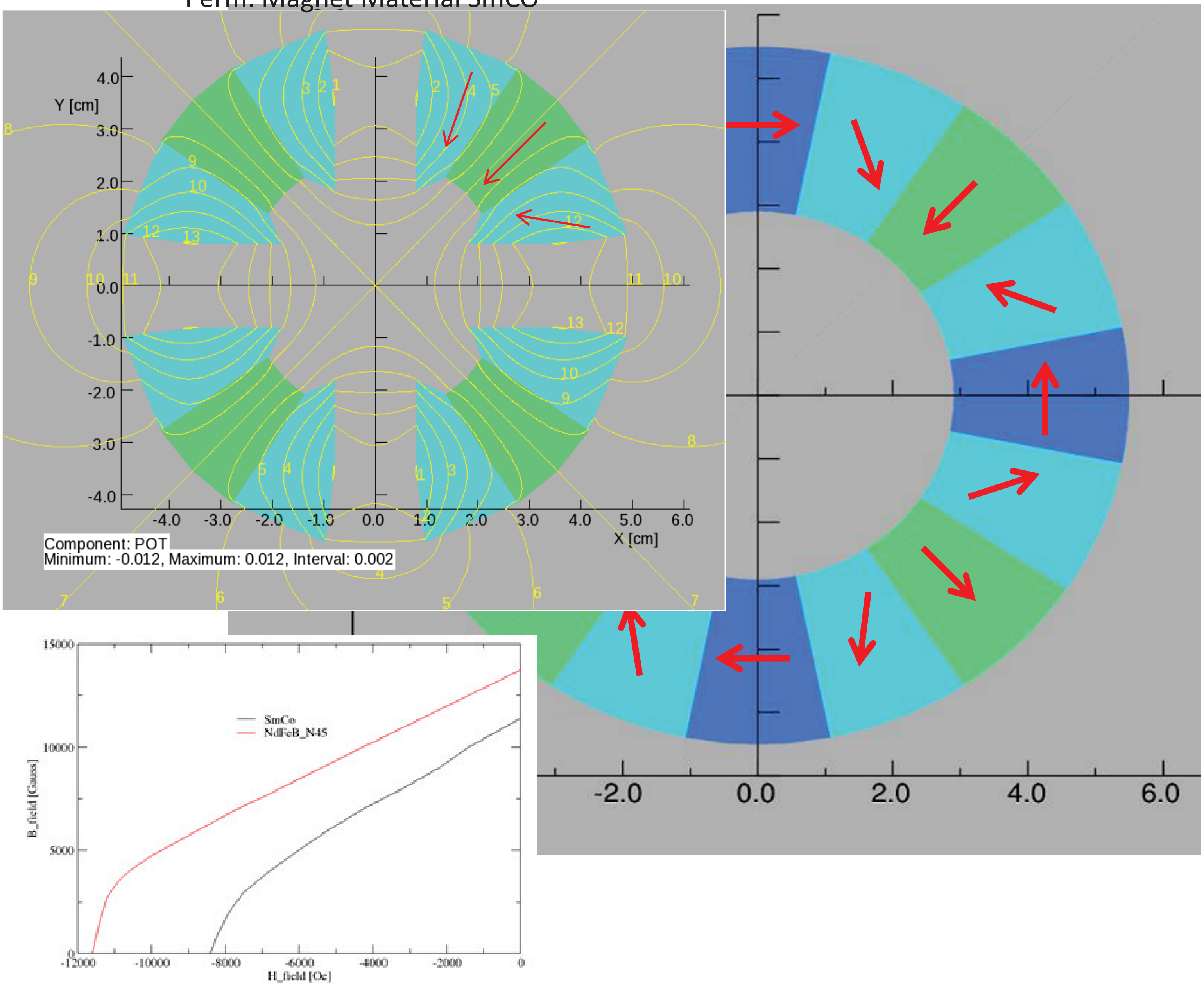

Perm. Magnet Material SmCO

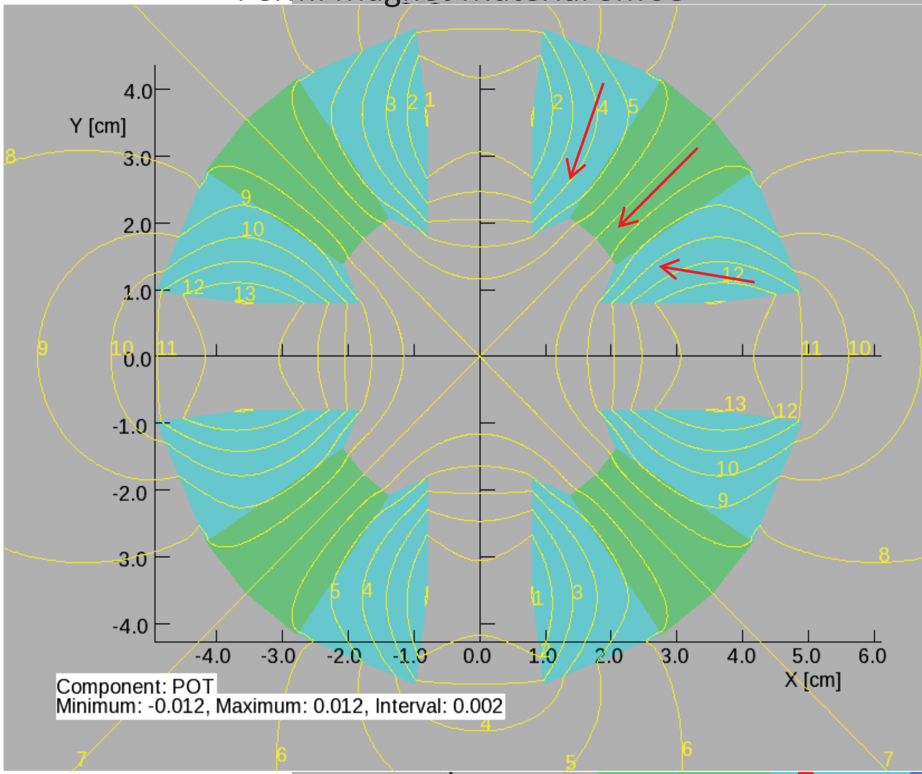

Perm. Magnet Material NdFeB

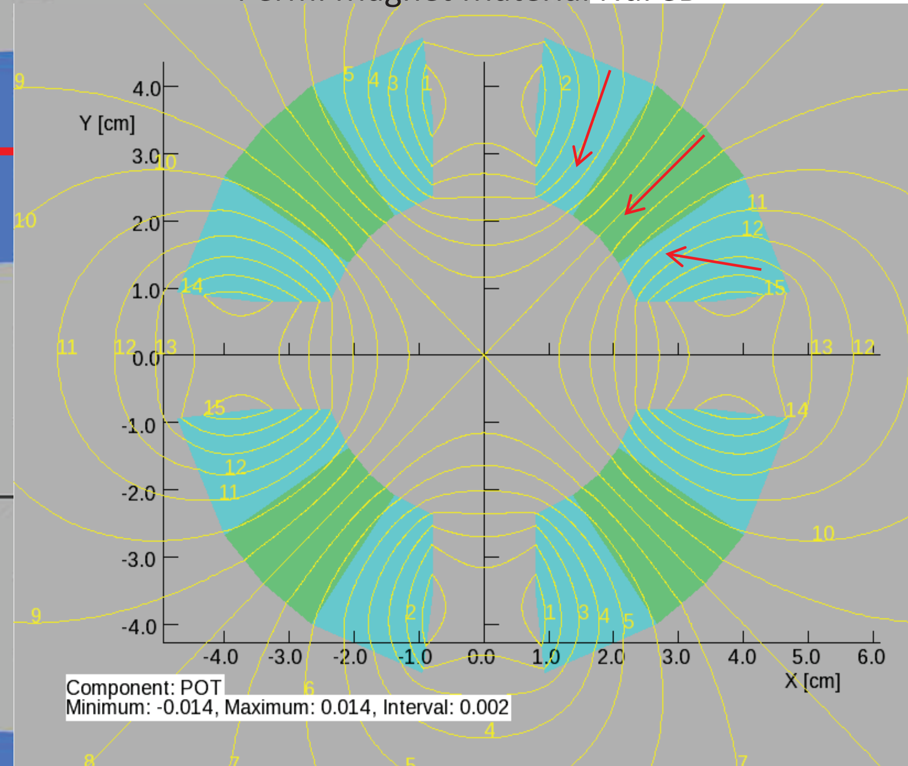

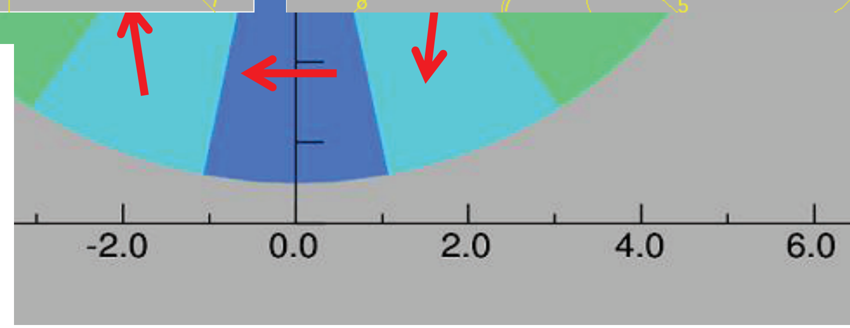

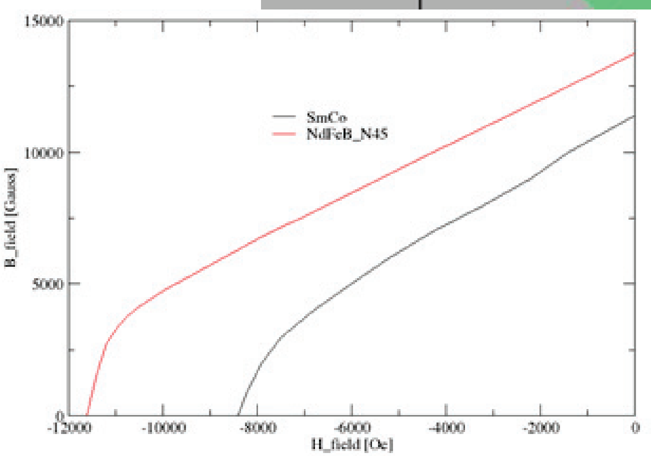

Perm. Magnet Material SmCO

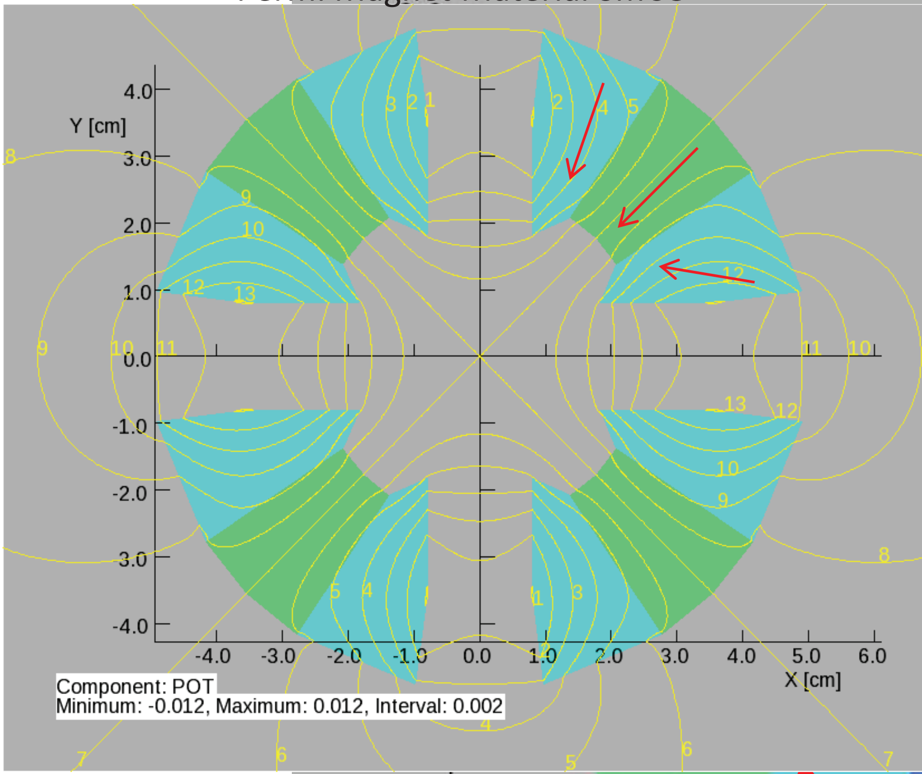

Perm. Magnet Material NdFeB

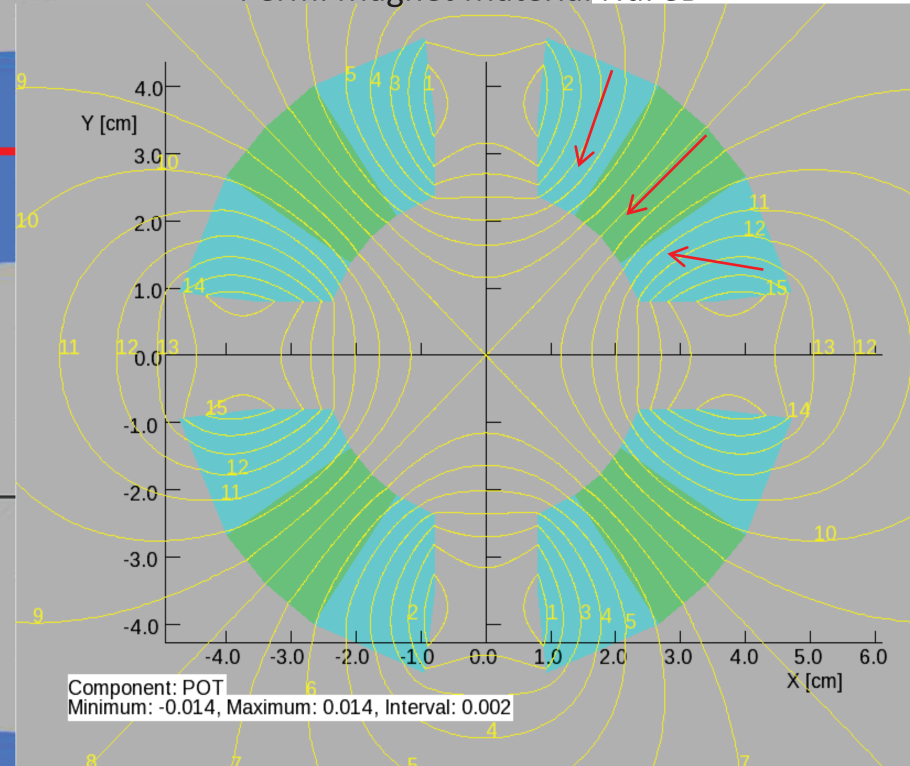

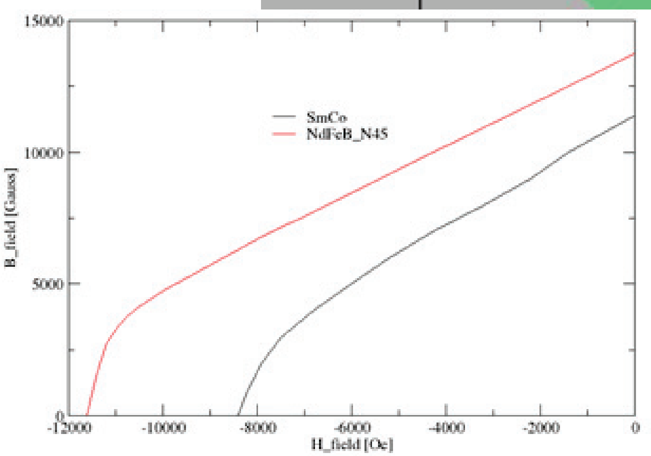

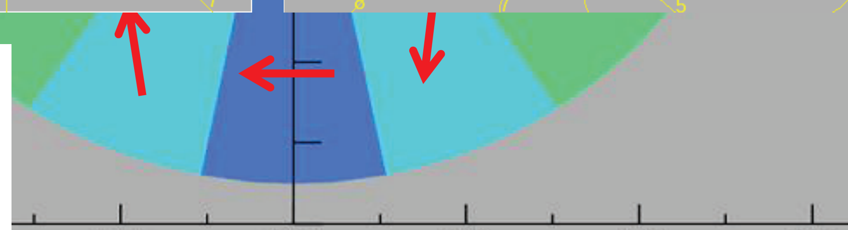

2D Design establishes the magnet's cross section

-The 12pole multipole=0 for R=1 cm

-NdFeB-N45 allows for larger inner radius

Schematic diagram of 3 consecutive FFAG cells

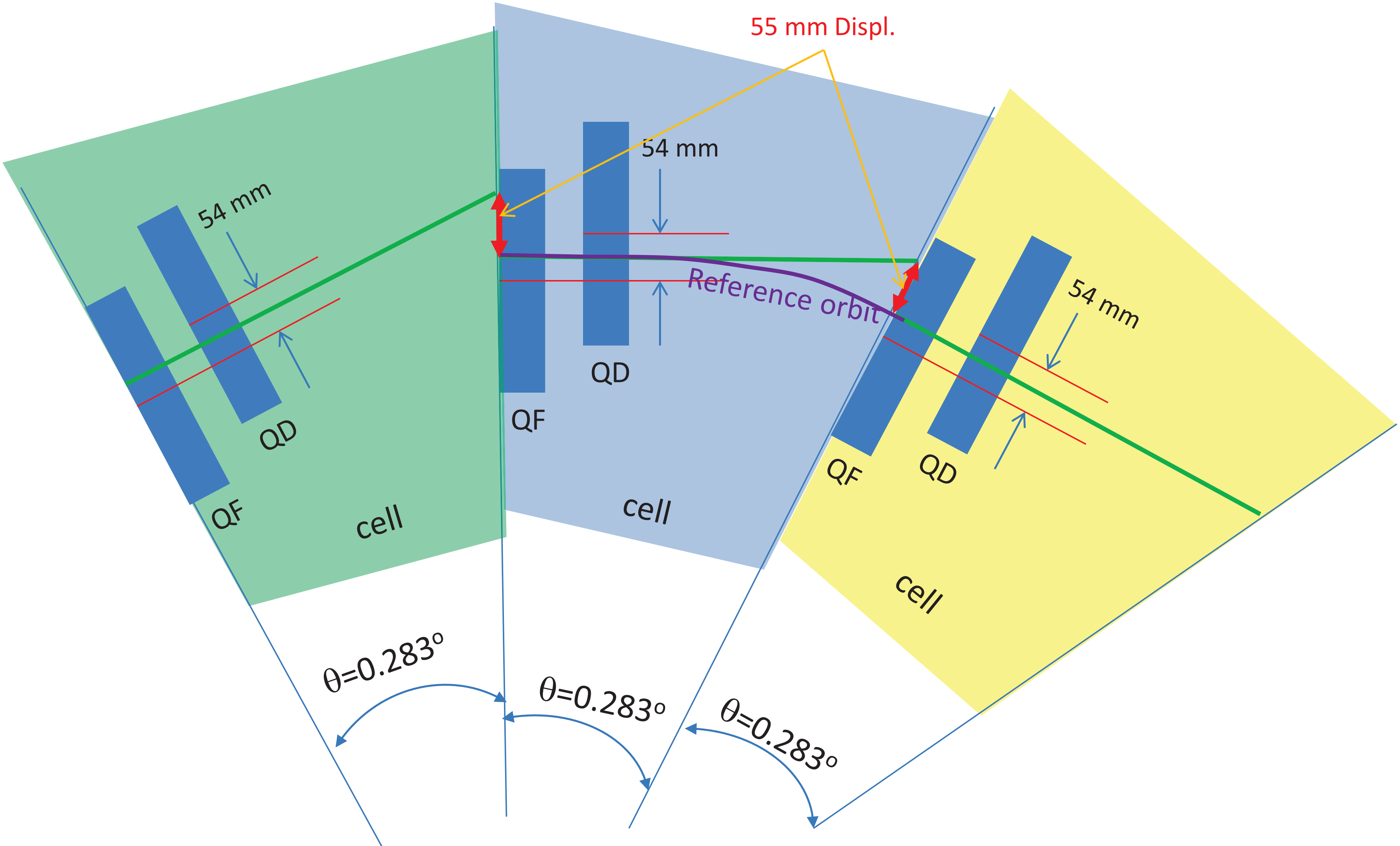

3D Magnetic field calculations for the FFAG cells

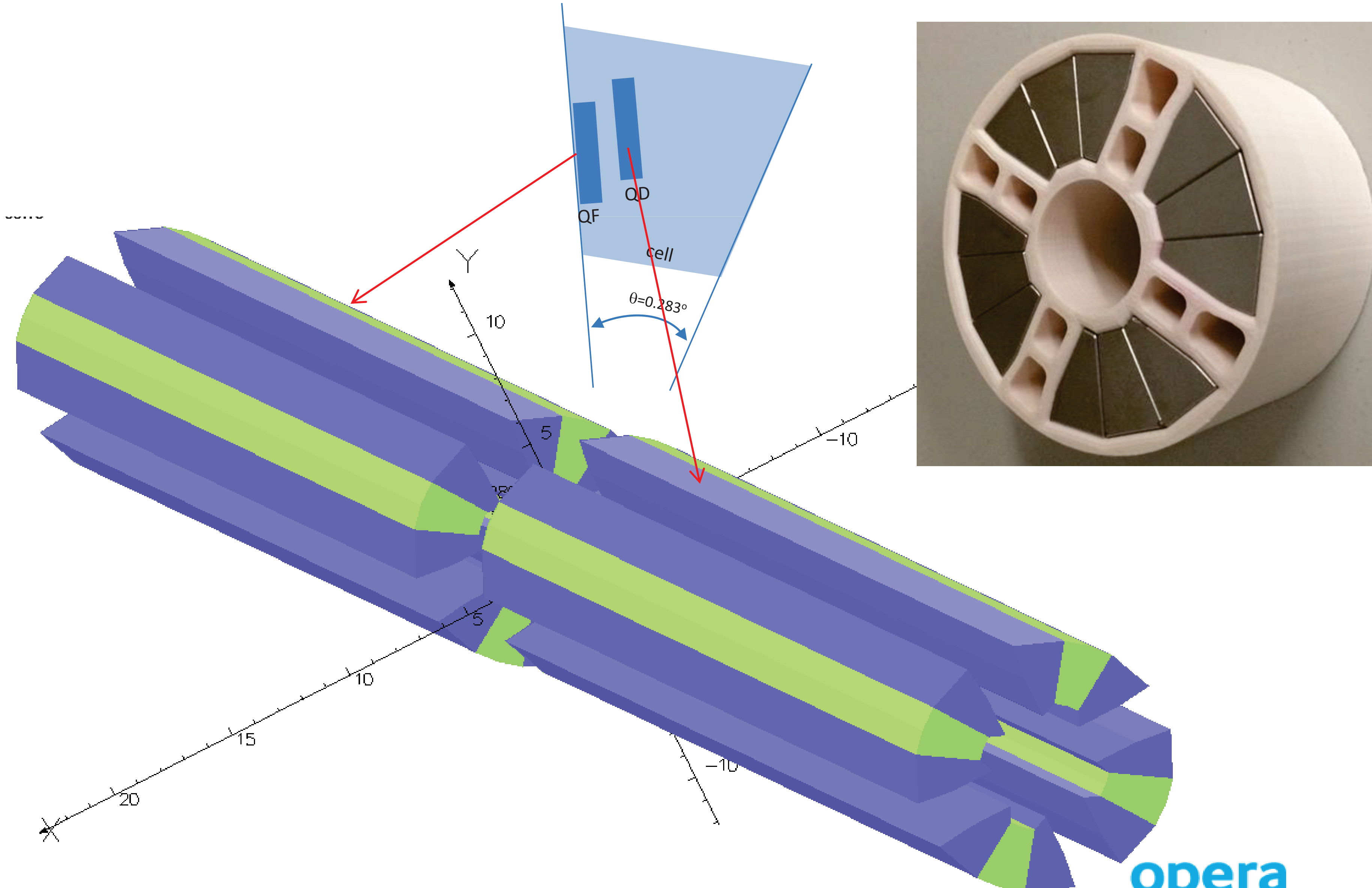

3D Magnetic field calculations for the FFAG cells

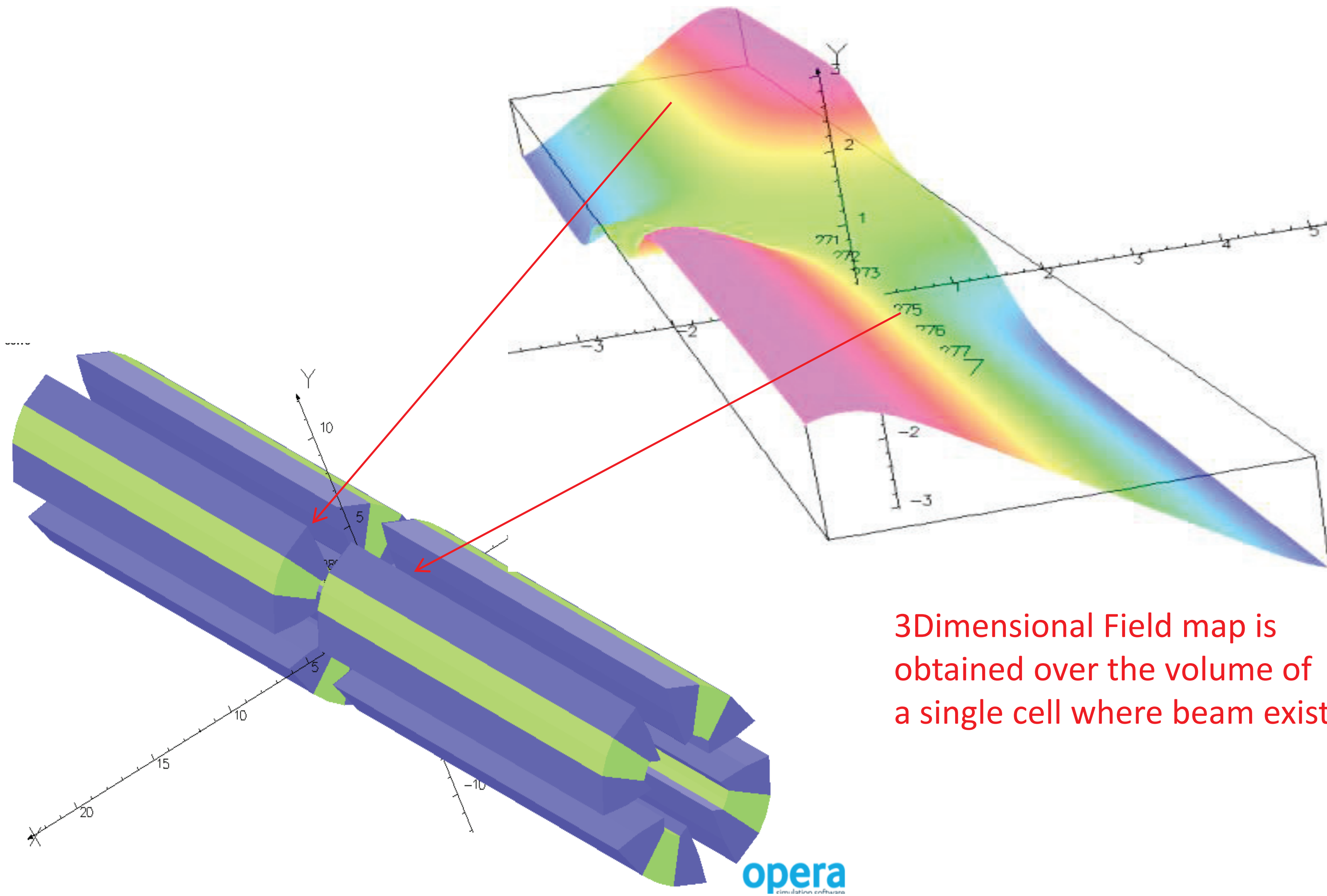

3Dimensional Field map is obtained over the volume of a single cell where beam exists.

Long coil measurement of the magnetic multipoles at R=1 cm

$$B_r(r,z,\theta) = \sum_{n=0}^{14} B_n(r,z)\sin((n+1)\theta) + \sum_{n=0}^{14} A_n(r,z)\cos((n+1)\theta)$$

$$\int_{-\infty}^{\infty} B_n(r,z)dz = \int_{-\infty}^{\infty} b_n(z)dz\left(\frac{r}{r_0}\right)^n \qquad \int_{-\infty}^{\infty} A_n(r,z)dz = \int_{-\infty}^{\infty} a_n(z)dz\left(\frac{r}{r_0}\right)^n$$

	$\int_{-\infty}^{+\infty} B_1(r,z)\cdot dz$ [Gauss]	Q_Diff/Q_{meas}	$\int_{-\infty}^{+\infty} B_5(r,z)\cdot dz$ [Gauss.cm^{-4}]	$12p\_diff/Q_{meas}$
SmCo R26HS Temp.=20º Calculations	18730.5		337.4	

Summary of field measurements in eRHIC Permanent Magnet Quadrupoles

Field harmonics are in "units" of 10^{-4} of the quadrupole field at a reference radius of 10 mm.

Note: Data in PMQ_0002 are processed to correspond to a magnet orientation that gives a negative integrated gradient, and nearly cancels the normal sextupole in PMQ_0001

Quantity	PMQ_0001	PMQ_0002
Integrated Gradient (T)	1.8647	-1.9096
Normal Dipole	--	--
Normal Quadrupole	10000.00	-10000.00
Normal Sextupole	27.83	-29.71
Normal Octupole	5.39	3.27
Normal Decapole	-4.92	0.07
Normal Dodecapole	-188.14	194.56
Normal 14-pole	-1.59	0.27
Normal 16-pole	-0.44	0.22
Normal 18-pole	-0.24	0.30
Normal 20-pole	-2.37	2.88
Normal 22-pole	0.04	0.02
Normal 24-pole	0.02	-0.01
Normal 26-pole	0.02	-0.02
Normal 28-pole	0.11	-0.12
Normal 30-pole	0.00	0.00

Theory 180.1

Quantity	PMQ_0001	PMQ_0002
Field Angle (mr)	--	--
Skew Dipole	--	--
Skew Quadrupole	--	--
Skew Sextupole	-16.41	-1.95
Skew Octupole	-12.32	0.50
Skew Decapole	-11.98	-0.24
Skew Dodecapole	-2.27	-1.03
Skew 14-pole	1.93	0.03
Skew 16-pole	-0.22	-0.06
Skew 18-pole	0.03	-0.18
Skew 20-pole	0.08	-0.01
Skew 22-pole	0.02	-0.03
Skew 24-pole	0.01	0.00
Skew 26-pole	0.00	0.01
Skew 28-pole	0.00	-0.01
Skew 30-pole	0.00	0.00

Summary_PMQ_0001_0002_20150406.xlsx Sheet1 *4/6/2015 11:44 AM*

The Optics of the Low Energy FFAG cell*

3D Field Maps were obtained from the 3D EM Calculations

- Calculate the closed orbits in the range 1.3 GeV to 6.6 GeV
- Calculations of tunes Q_x,Q_y and chromaticities ξ_x, ξ_y per cell.
- Calculations of the maximum beam emittances ε_x, ε_y transported in the low energy arc for each of the five orbits.
- Calculation of the dynamic aperture of the transport ring.
- Calculation of the beta functions.

* The zgoubi computer code was used in the calculations.

Closed orbits in the range 1.3 GeV to 6.6 GeV

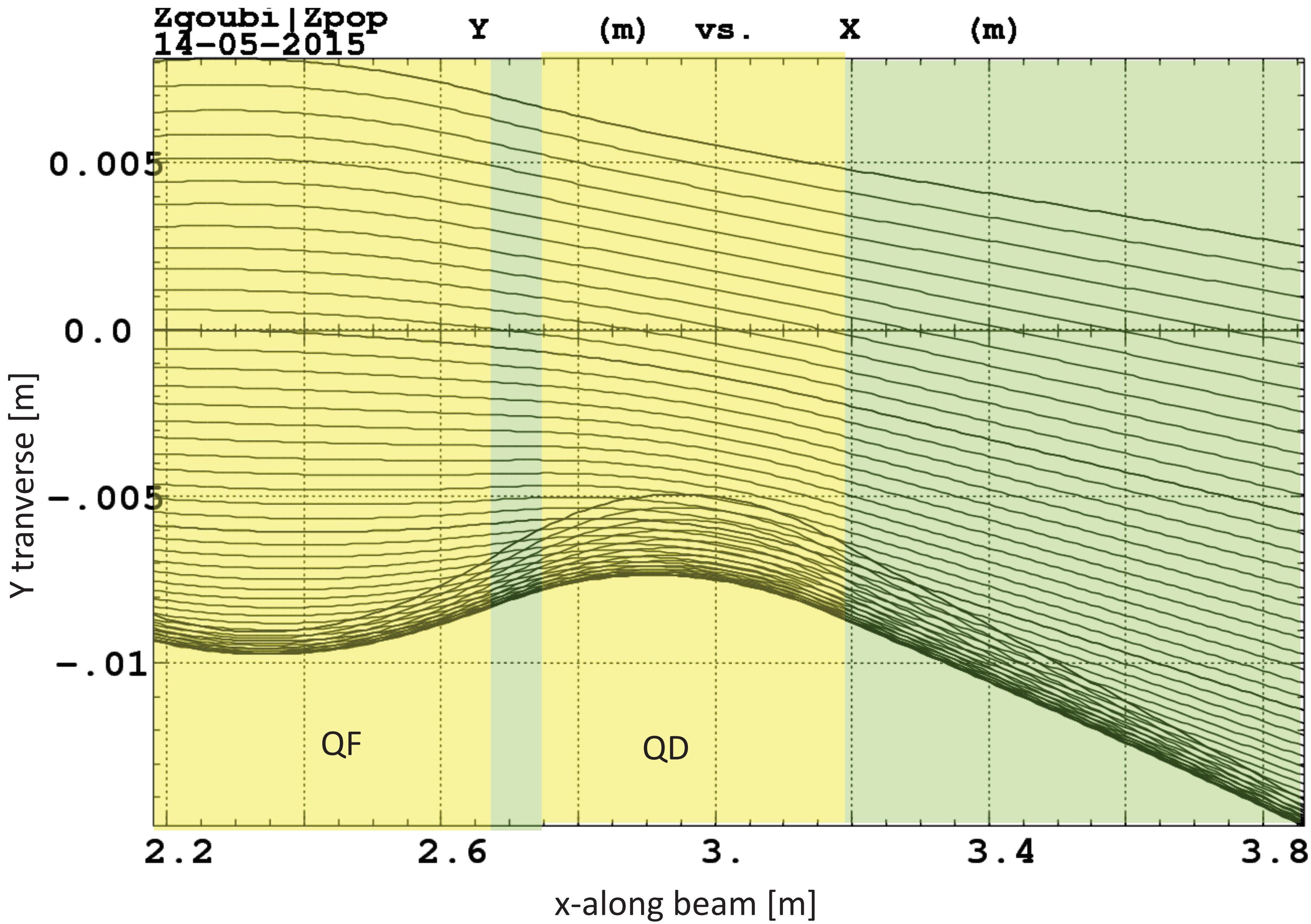

Tunes Q_x,Q_y and chromaticities ξ_x, ξ_y; Range: 1.3 GeV to 6.6 GeV

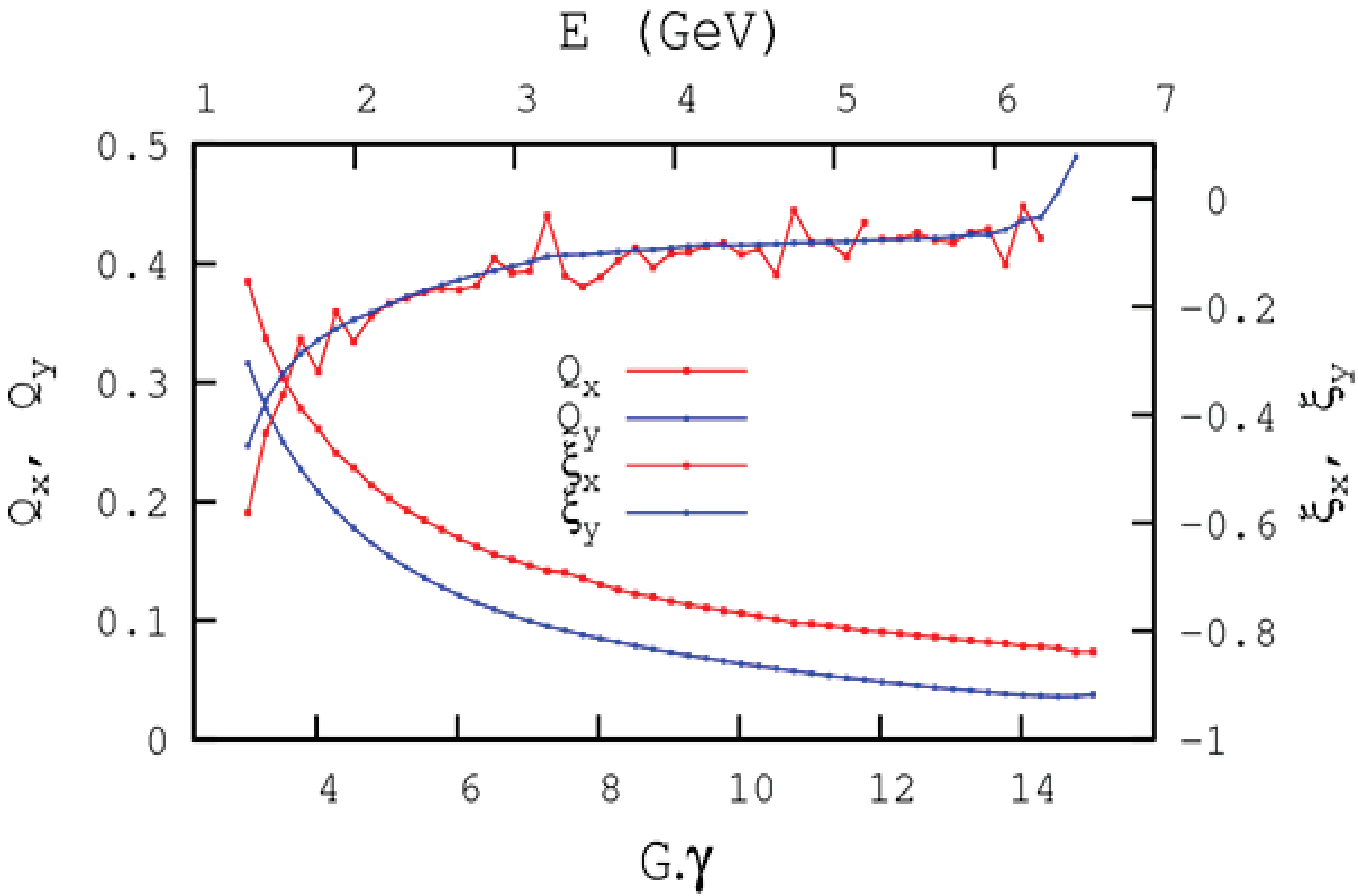

Calculations of the maximum beam emittance ε_x transported in all six arcs for each of the five orbits.

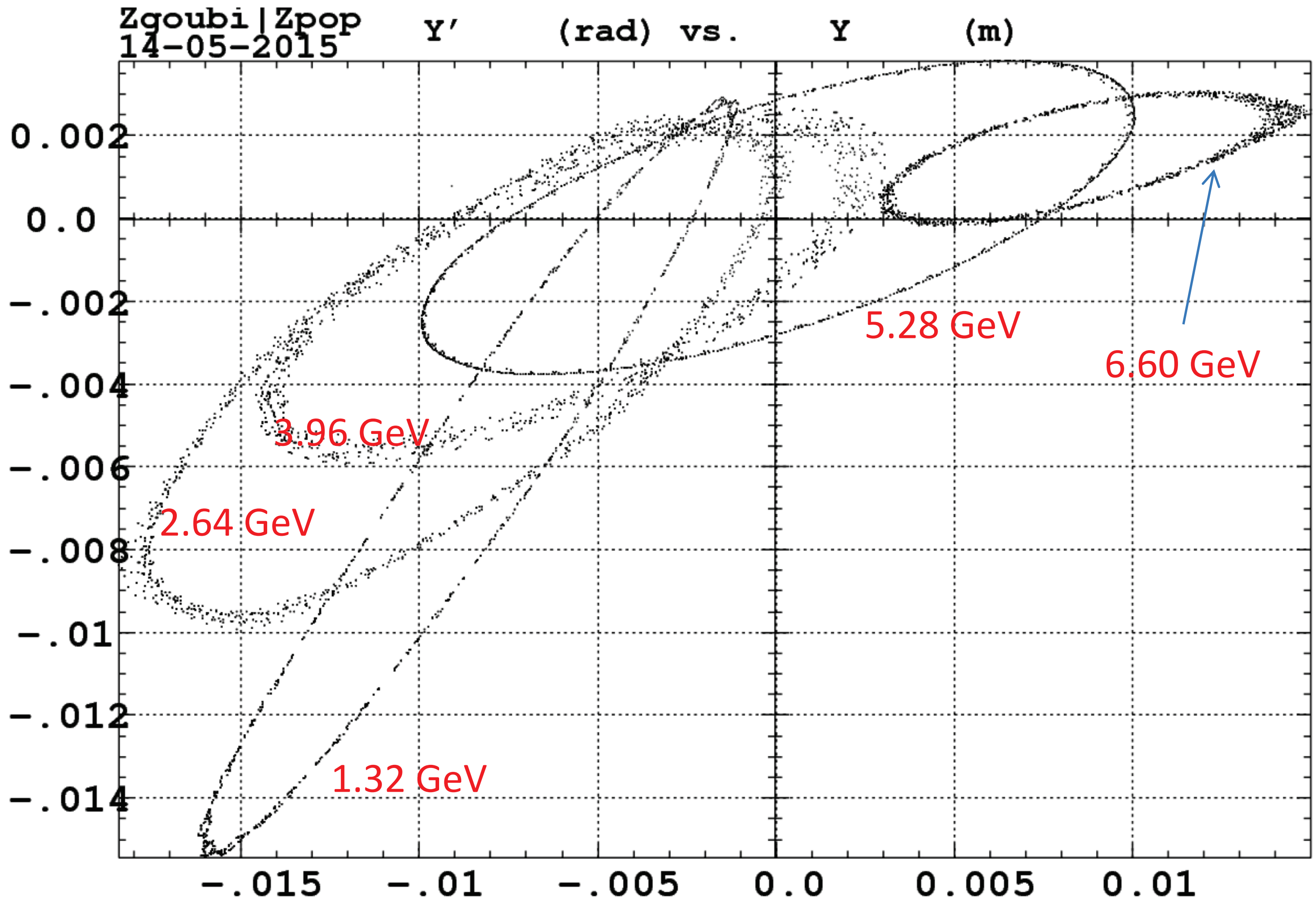

Calculations of the maximum beam emittance ε_x transported in all six arcs for each of the five orbits.

Max_$\varepsilon_{N\text{-}rms}$=0.02 m.rad

Required_$\varepsilon_{N\text{-}rms}$ to be transported=30×10^{-6} m.rad

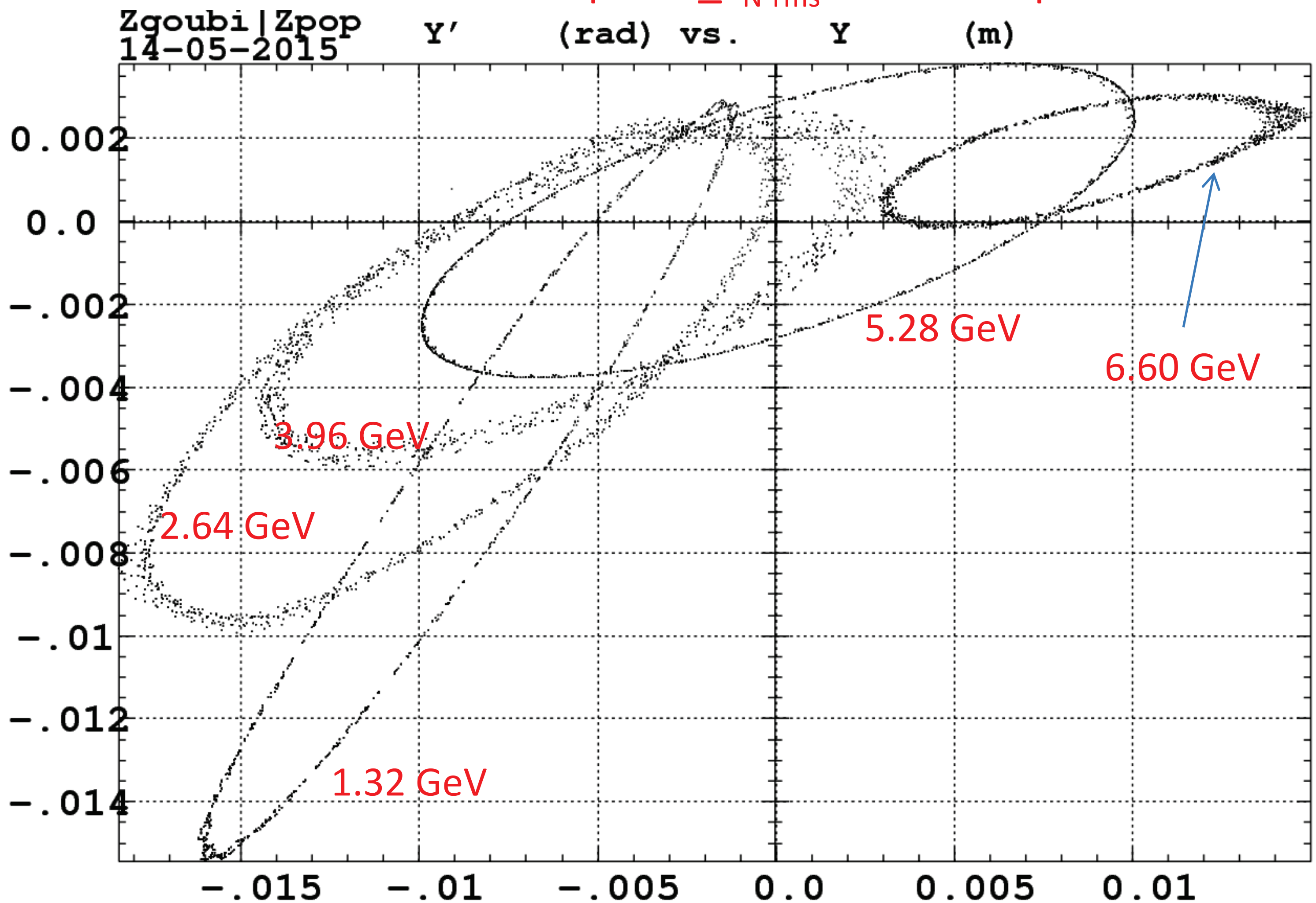

Calculations of the maximum beam emittance ε_y transported in all six arcs for each of the five orbits.

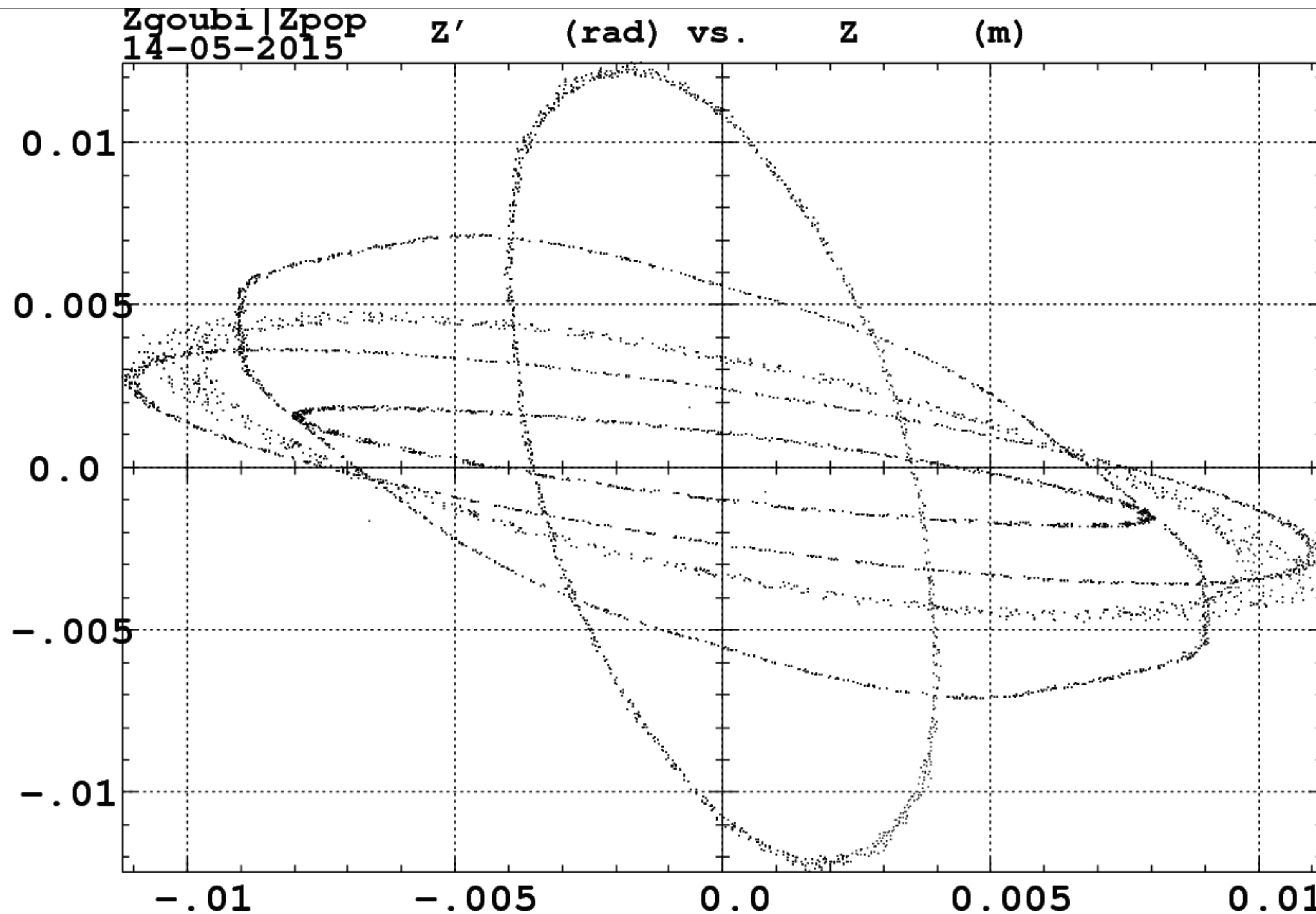

Calculations of the maximum beam emittance ε_y transported in all six arcs for each of the five orbits.

Max_$\varepsilon_{N\text{-}rms}$=0.02 m.rad

Required _εN-rms to be transported=30x10^{-6} m.rad

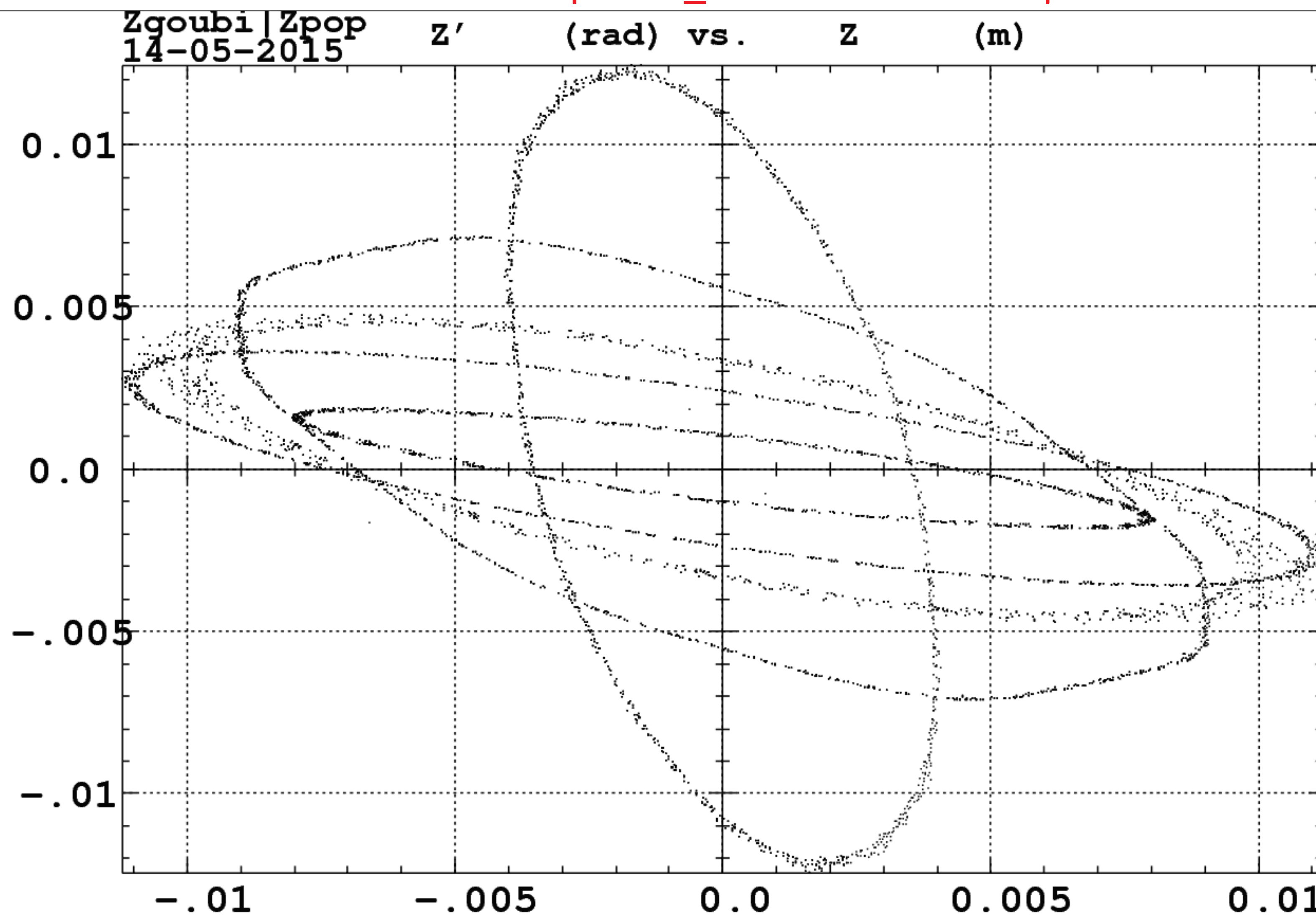

The dynamic aperture at the exit of 1000 cells

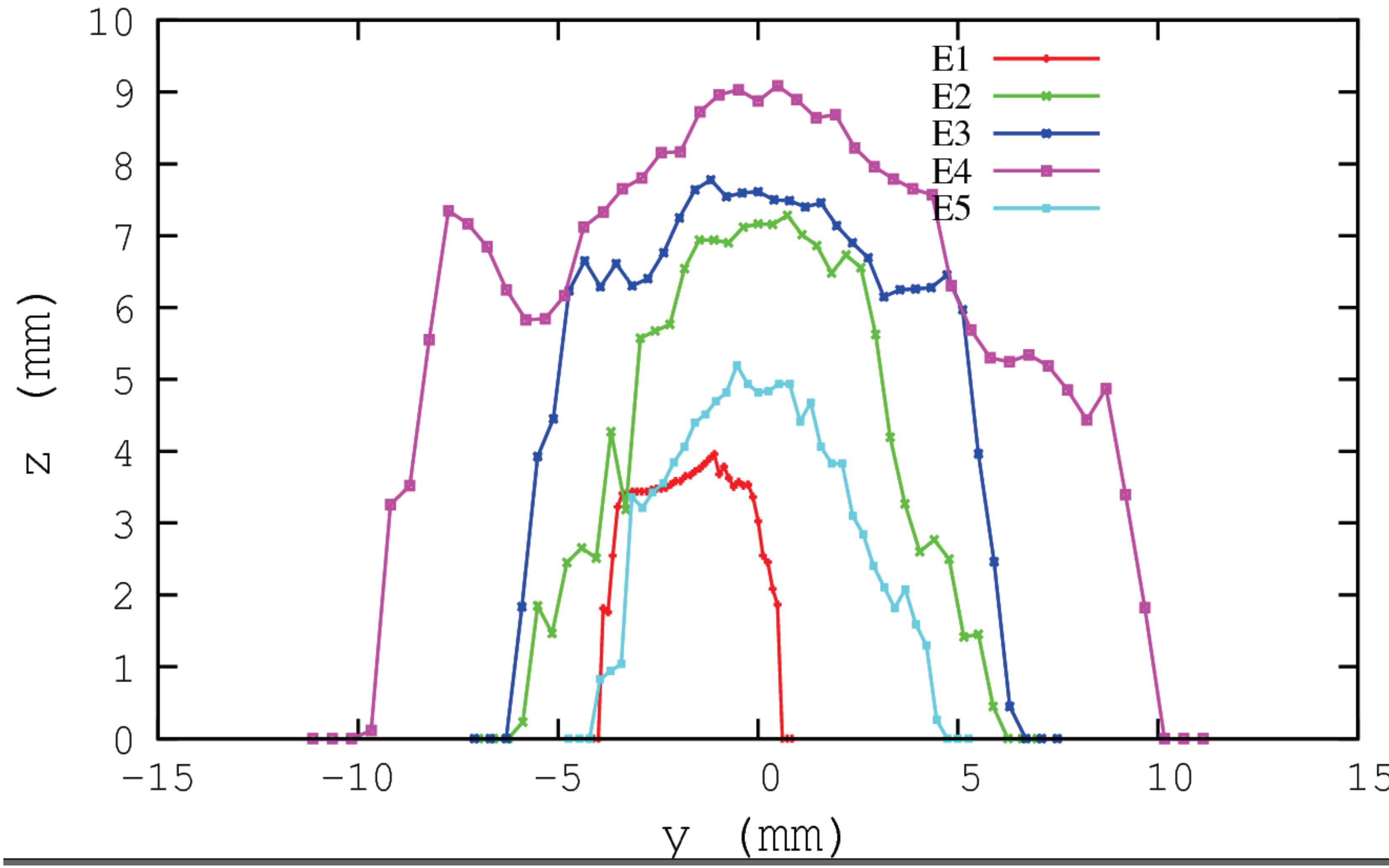

Beta functions of 3 different energies

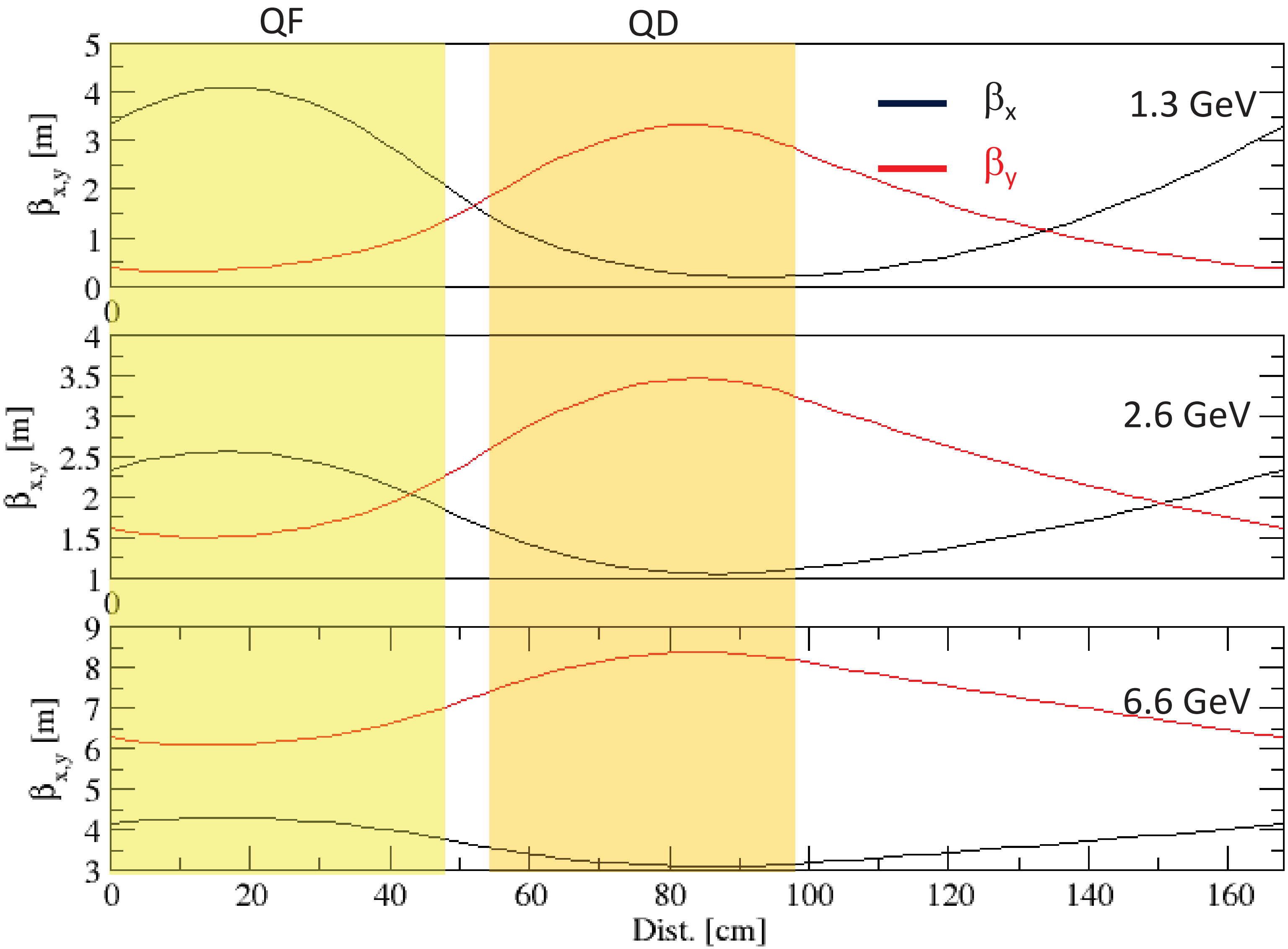

Conclusions

- The results from the calculations on the beam optics of the low energy cell meet well the requirements.

- The calculated 3D magnetic fields of a single magnet are in good agreement with the measurements.

THE END

THANK YOU FOR YOUR ATTENTION

How can we correct for the multipoles? Method II

Change the direction of wedge's-easy-axis by $\Delta\phi \propto \dfrac{multipole - error}{\sin\phi}$

$$\Delta(\cos\phi) \propto multipole - error$$

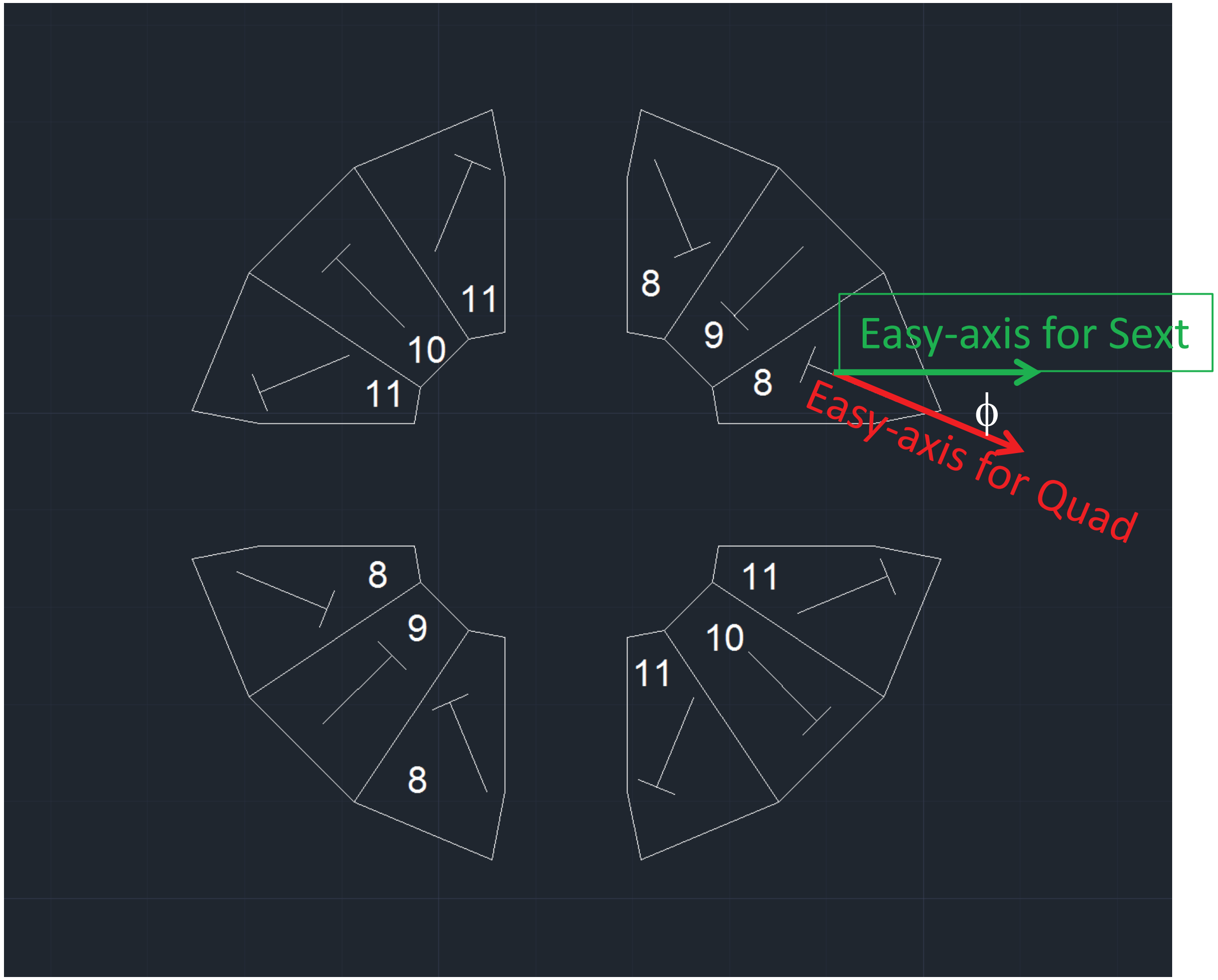

How can we correct for the multipoles? Method II

Change the direction of wedge's-easy-axis by $\Delta\phi \propto \dfrac{multipole - error}{\sin\phi}$

$$\Delta(\cos\phi) \propto multipole - error$$

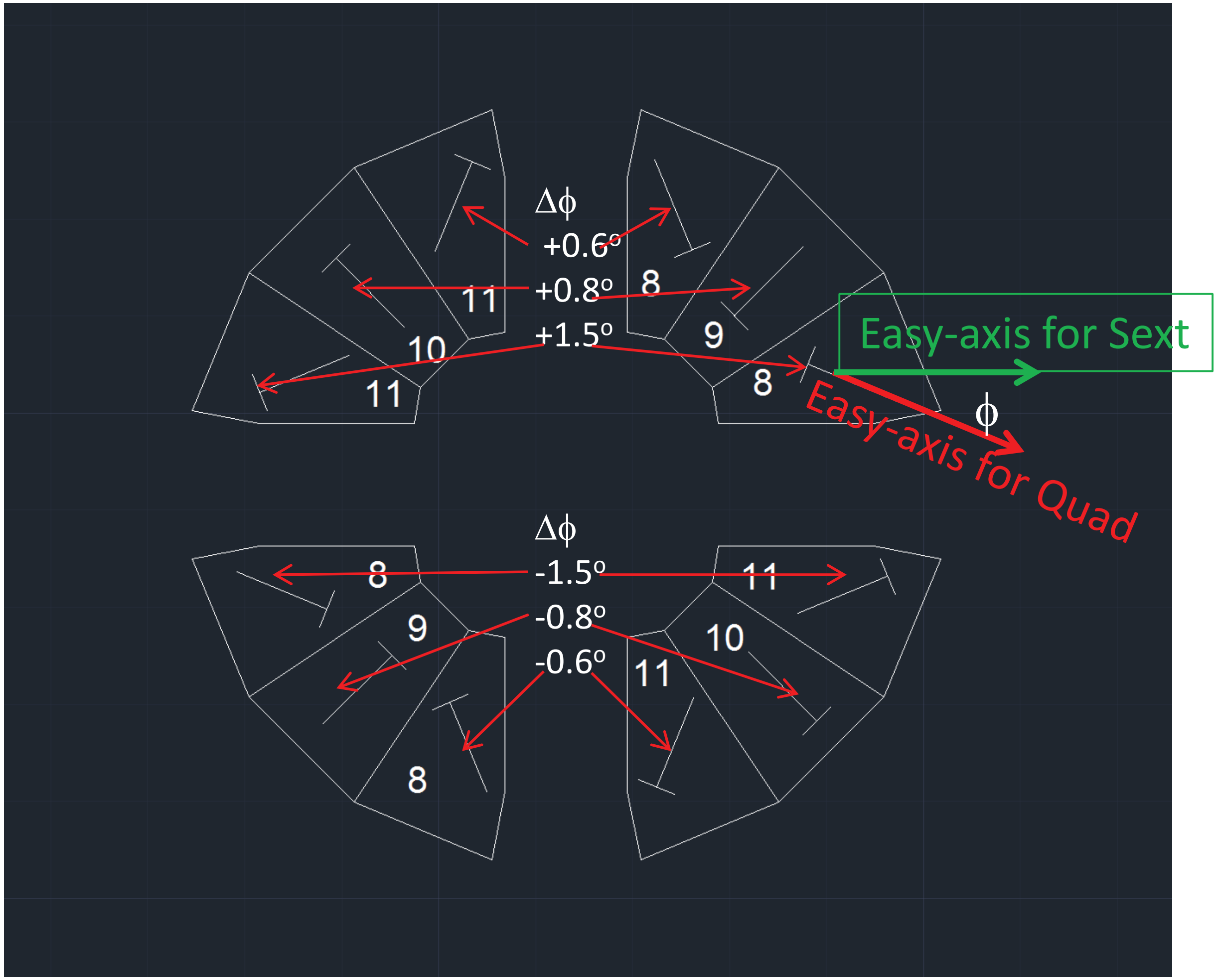

How can we correct for the multipoles?

Method II

Change the direction of Rod's-easy-axis by

$$\Delta(\cos\phi) \propto multipole - error$$

$$\Delta\phi \propto \frac{multipole - error}{\sin\phi}$$

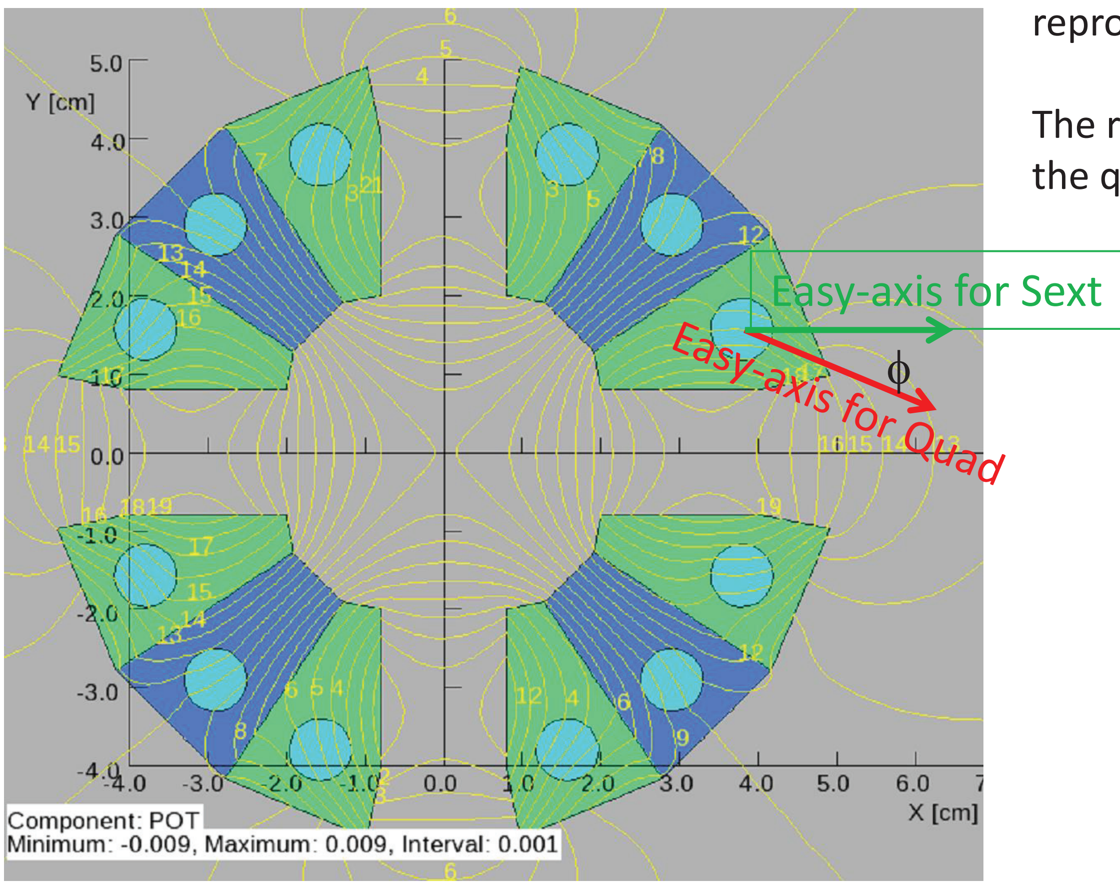

Either method can "easily" reproduce the measure sextupole

The rest of the multipole including the quad remain practically unchanged

How can we correct for the multipoles?

Method II

Change the direction of Rod's-easy-axis by

$$\Delta\phi \propto \frac{multipole - error}{\sin\phi}$$

$$\Delta(\cos\phi) \propto multipole - error$$

Either method can "easily" reproduce the measure sextupole

The rest of the multipole including the quad remain practically unchanged

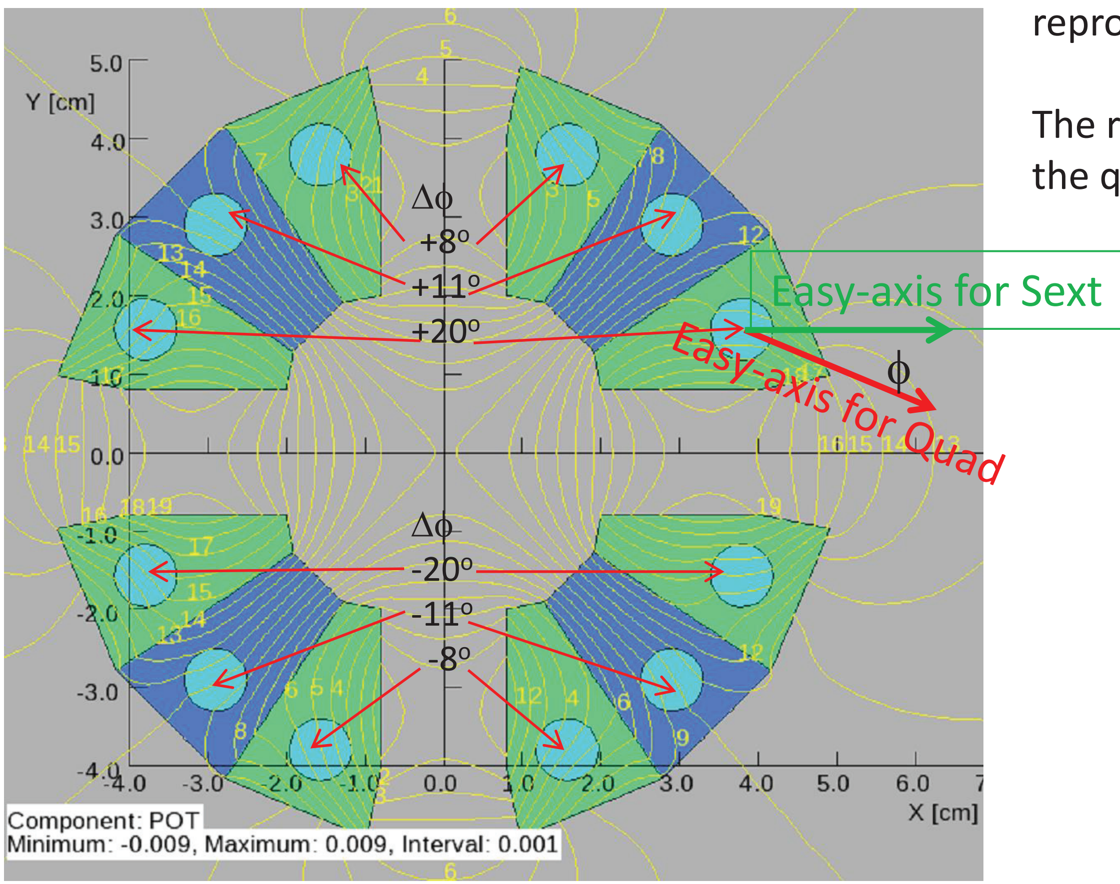

How can we correct for the multipoles? Method III

Use surface-current coils